Scientia Iranica B (2023) 30(6), 1987–2000

SCIENTIA IRANICA

Sharif University of Technology
Scientia Iranica
Transactions B: Mechanical Engineering
http://scientiairanica.sharif.edu

Research Note

Multi-objective optimization of machining parameters on aluminum alloy metal matrix composites using response surface methodology

P. Lakshmikanthan[a,*], K. Senthilvel[b], and B. Prabu[c]

a. *Department of Mechanical Engineering, University College of Engineering, Panruti, Tamilnadu-607106, India.*
b. *Department of Mechanical Engineering, Karaikal Govt. Polytechnic College, Karaikal, Puducherry, India.*
c. *Department of Mechanical Engineering, Puducherry Technological University, Puducherry, India.*

Received 23 January 2022; received in revised form 15 August 2022; accepted 21 February 2023

KEYWORDS
LM13;
RHA;
CCD;
Surface roughness;
MRR;
RSM.

Abstract. Due to their lightweight, new classes of materials, including aluminum-based Metal Matrix Composites (MMCs), have been popular in recent years in various industries, including aircraft and automobiles. Because of its low cost and ease of availability, aluminum alloy (LM13) MMCs were developed using Rice Husk Ash (RHA) as reinforcement in this study rather than traditional reinforcement, and composites were prepared using the stir casting technique. LM13-15wt.%RHA composite was chosen for the present machining study. The Central Composite Design (CCD) with three input parameters at three levels based on the best outcomes was adopted for this experimental study. A mathematical model was developed to predict the machining responses of Material Removal Rate (MRR) and surface roughness. The most significant variables were evaluated using ANOVA. The main and interactive effects of the input variables on the predicted responses are determined. The experimental and predicted values are nearly identical, indicating that the developed models can accurately predict responses. The optimal value of the turning parameters was obtained from desirability analysis. The obtained desirability value for turning parameters is 0.863, and for output response, the desirability value for surface roughness and MRR is 0.71663 and 0.747491, respectively, and the combined desirability is 0.731898.

1. Introduction

The emergence of new composite materials is continually evolving the engineering market globally and expanding their use in most engineering applications such as cylinder block linear, automotive pistons, calipers, bicycle frames, etc. Composite materials are currently piquing the interest of researchers owing to their admirable mechanical attributes. Metal Matrix Composites (MMCs) have excellent impact resistance, tensile strength, and wear resistance. Composites are more extensively used than traditional materials because of their adaptability in extending mechanical properties [1]. Aluminum matrix composites have developed a firm place in the lightweight materials

*. *Corresponding author.*
E-mail addresses: lakanpec@gmail.com (P. Lakshmikanthan); sensukikrishna@gmail.com (K. Senthilvel); prabu@pec.edu (B. Prabu)

doi: 10.24200/sci.2023.59821.6445

category due to a wide range of desirable properties, including low density, good wear resistance, and corrosion resistance [2,3].

Many researchers and authors [4–7] have worked and reported the considerable benefits of Al-MMC and MMC compared to well-known conventional engineering materials. Due to their immense availability and cheap nature, agricultural products and by-products have been explored as noteworthy reinforcement constituents. As a result, several researchers have looked at various farming wastes and discovered they are high in silicon and magnesium oxide elements, among other things [8]. Coconut shell, corn cob, groundnut shell, bagasse, and rice husk are some of the well-known agro wastes.

It was demonstrated by several researchers that conventional agricultural waste such as rice husk, coconut shell ash, fly ash, corn cob ash, red mud, and other agricultural wastes could all be employed as potential enhancers for aluminum-based composites. Ash from rice husks belongs to this category, and it's a waste by-product from agriculture that's readily available. This waste product is created from rice husks and is widely available as an agricultural waste by-product. As a result, researchers are working to discover ways and means to utilize this agricultural waste effectively. According to current research, Rice Husk Ash (RHA) includes between 85 and 90% amorphous silica [9]. This silica converts into cristobalite, which is crystalline in nature when heated. However, if the heating temperature is controlled in the furnace, amorphous silica may occur. This manufactured material usually has a high surface area, a fine size, and a high reactivity. Consequently, micro-silica can be used to make advanced materials such as SiC, elemental Si, Mg_2Si, and Si_3N_4 [10]. As a result, it is crucial to explore ways to make aluminum-reinforced RHA composite materials for numerous structural and engineering utilisations such as automotive, aerospace, and sporting goods. Hence, studying such materials' machining has become vital and highly compelling [11].

The complications of machining MMCs have been examined in further depth from a variety of perspectives. The reinforcing phase's shape, volume fraction, and distribution, as well as the matrix traits, are the utmost indispensable aspects influencing the entire machining process, according to the existing research on particulate MMCs [12]. One of the most crucial considerations that affect composites' practical application is their machined surface quality. Several researchers have experimented with MMC machining. Sahin et al. [13] have stated the dominant influence of input speed on surface roughness. Parameters like cutting speed, depth of cut, feed, cutting fluid, and rake angle influence chip shape, forces, wear, Material Removal Rate (MRR), and surface roughness, according to Hocheng et al. [14].

When machining MMC, the main problem is inordinately excessive tool wear; ceramic fibers or particles produce an abrasive effect. Thus, materials with exceptional abrasion resistance are frequently endorsed [15]. High Speed Steel (HSS) tools are insufficient for rough machining; cemented carbide tools are used for rough machining, and Polycrystalline Diamond (PCD) tools are used for finish machining [16]. Because PCD tools are expensive, it is required to conduct fundamental machinability studies to identify machining parameters for carbide tools that will result in high output at a reasonable cost.

Several investigations on Al-MMC machining suggest that maximizing MRR and reducing surface roughness is challenging and must be managed. The preeminent intent of this investigation is to understand how machining parameters affect the MRR and surface finish of L13-RHA MMC in the process of turning. During turning L13-RHA composites under roughing conditions, three primary cutting parameters were selected (cutting speed, feed rate, and cut depth) and tuned to maximize MRR and minimize surface roughness. For Central Composite Design (CCD), ANOVA was used to determine the values of cutting parameters that optimize these response variables. For predicting surface roughness, a mathematical model was created using Response Surface Methodology (RSM). Measured and predicted values are highly consistent, demonstrating the model's efficacy in predicting surface roughness on the machining of L13-RHA composites.

2. Materials and methods

2.1. Materials

Aluminum alloy LM13 was selected as the matrix material, and RHA powder with a mesh size of less than 120 μm was chosen as the reinforcement. According to Alaneme's directions [17], RHA was synthesized by thoroughly burning rice husks, thermal processing, and sieving afterward. The X-Ray Fluorescence (XRF) spectroscopy analysis was carried out. As determined by XRF, RHA's chemical composition is presented in Table 1. The primary elements of the ash were confirmed by XRF analysis to be SiO_2, Al_2O_3, and

Table 1. The chemical composition of RHA.

Element	SiO_2	Al_2O_3	Fe_2O_3	Cr_2O_3	CaO	MgO	K_2O	Others
Wt.%	38.12	26.52	17.38	6.34	1.59	1.61	0.40	Remaining

Fe_2O_3. The inclusion of hard substances (SiO_2, Al_2O_3, and Fe_2O_3) in the ash indicates that it contains hard substances [17,18]. Other oxides (Na_2O, K_2O, and MnO) were also detected in trace amounts. The presence of hard components indicates that RHA could be employed as a particle-reinforcing material.

2.2. Methods

The materials and casting technique are explained in detail elsewhere [19]. Stir casting was used to produce composites containing 0, 3, 6, 9, 12, and 15wt.%RHA. At 750°C, the aluminum alloy LM13 was molten. A graphite stirrer was used to stir this melt at a speed of 450 rpm. During stirring, Particles of the preheated RHA were slowly added to the melt in the form of pellets. Hexachloroethane (C_2Cl_6) tablets were included to degas the molten metal and eliminate the entrapped gases and other impurities. After completing the RHA particle mixing, the melt was put into the preheated mold and allowed to solidify. The hardness of the material was measured using the ASTM E10 standard on the manufactured specimens by Brinell hardness equipment (a Wilson instruments hardness tester). In addition, mechanical characteristics were assessed using UTM in accordance with ASTM E8. The Scanning Electron Microscope (SEM) was used to verify that the reinforcement in the composite was distributed uniformly.

3. Response Surface Methodology (RSM)

A statistical and mathematical tool for examining and assessing the behavior of a data set since the fit of a polynomial equation is known as the response surface technique. When numerous variables influence a response or a collection of responses of concern, this strategy can be useful. The second-order polynomial model was created to link the selected parameters to the answer, Eq. (1):

$$y = a_0 + \sum_{K-1}^{i} a_i x_i + \sum_{k-2}^{i} a_{ii} x^2 + \sum a_{ii} x_i x_j + \alpha. \quad (1)$$

The coefficients ai of Eq. (1) are determined by least square fitting of higher order response surface model for controllable process parameters (x_i) values, and using this model, response optimization can be carried out.

The linear, higher-order, and interaction effects are represented by the second, third, and fourth terms, respectively, in the constructed model [20,21]. The CCD under RSM was preferred in the Design-Expert 8.0 statistical software for choosing the set of experiments and the objective. The tally of the experiments chosen is determined by the count of parameters for each test. Based on the literature survey [22,23], the three parameters selected for the trials were the cutting speed, feed, and depth of cut, with MRR and surface roughness being the response. The three parameters are varied over the ranges of 750–1250 rpm, 0.1–0.2 m/rev, and 0.1–0.3 mm, respectively, and 20 experiments for LM13-15wt.%RHA composite have been generated, as shown in Table 2.

Table 2. Machining parameter factors and their levels.

	Level-1	Level-2	Level-3
Parameters	**−1**	**0**	**+1**
Cutting speed (RPM)	750	1000	1250
Feed (mm/rev)	0.1	0.2	0.3
Depth of cut (mm)	0.5	1	1.5

3.1. Central Composite Design (CCD)

CCD can be implemented in response surface technique to generate a second-order (quadratic) model for the response variable, obviating the need for a full three-level factorial design [24]. Most statistical software applications support three types of CCD: face-cantered, rotatable, and inscribed. To obtain adequate results, the specified experiment is carried out, and linear regression might be performed repeatedly [25].

3.2. Experimental designs

RSM is an excellent tool for enhancing, refining and developing quality. The number of trials in this study was calculated using RSM. The CCD response section is a full-factorial design with most of the parameter sequences at three stages (high 1, medium 1, and low −1). The CCDs have twenty experimental values at three input elements, and the output responses are calculated when the trials are completed. Table 3 lists the responses which have been recorded. Fitted summary output from the Design-Expert 8.0 program indicates a statistically significant endorsement for the quadratic model for further evaluation.

4. Result and discussion

4.1. Hardness test

Figure 1 presents the alteration in hardness with varying wt.% of RHA reinforcement. The hardness of the composite augments as the RHA content is enhanced from 0wt.% to 15wt.%. The formation of hard-ceramic phases in the ductile matrix phase, such as Al_2O_3, SiC, Fe_2O_3, and SiO_2 is responsible for such a large increase in hardness. With augmentation in RHA content, the proportion of brittle and hard phases in the matrix increases. The differing Coefficients of Thermal Expansion (CTE) of the brittle and hard reinforcement and the ductile and soft cause the matrix and reinforcement to become elastic and plastically incompatible, resulting in increased hardness. Similar findings were reported by Rajan et al. [26].

Table 3. Experimental designs and results.

Exp. run	Run order	Cutting speed (RPM)	Feed (mm/rev)	Depth of cut (mm)	Surface roughness (μm)	MRR (mm^3/s)
1	9	750	0.1	0.1	1.97	1005
2	8	1250	0.1	0.1	2.37	1260
3	2	750	0.2	0.1	2.89	1517
4	6	1250	0.2	0.1	2.98	1080
5	7	750	0.1	0.3	2.35	1548
6	12	1250	0.1	0.3	3.29	1910
7	1	750	0.2	0.3	2.78	2020
8	4	1250	0.2	0.3	3.42	1490
9	3	1000	0.15	0.2	2.63	1310
10	10	1000	0.15	0.2	2.61	1555
11	5	1000	0.15	0.2	2.65	1550
12	11	1000	0.15	0.2	2.65	1665
13	17	750	0.15	0.2	2.07	1660
14	13	1250	0.15	0.2	2.67	1585
15	20	1000	0.1	0.2	2.67	1625
16	16	1000	0.2	0.2	3.19	1380
17	15	1000	0.15	0.1	2.52	1505
18	18	1000	0.15	0.3	2.93	1600
19	14	1000	0.15	0.2	2.62	1590
20	19	1000	0.15	0.2	2.62	1680

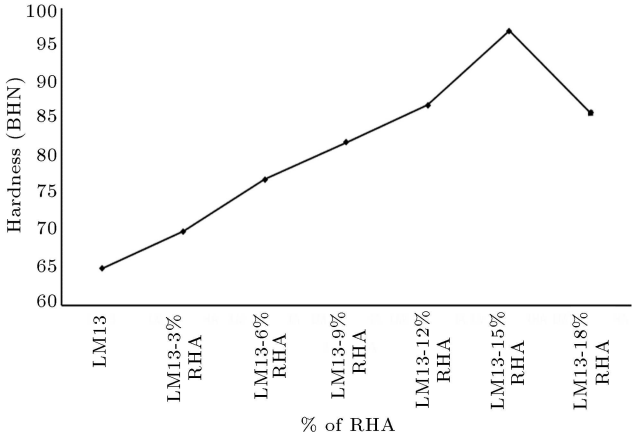

Figure 1. Hardness of LM13-RHA composite.

Hardness exhibits a maximum value at 15wt.% of RHA and further declines with increased RHA content. Because RHA has a low density, it takes up more space in the composite. The amount of reinforcement trapped in the matrix enhances with an increase in % of reinforcement. Consequently, the reinforcement-matrix interaction decreases while the interaction between the reinforcement particles with poor wettability increases, providing a cushioning effect with the matrix particles and reducing hardness [27].

4.2. Tensile and yield strength

Figures 2 and 3 demonstrate the tensile strength and yield variations of composites with varied RHA particle wt.%. The ultimate tensile strength of composites improves to a higher value as RHA is increased from 0% to 15%. The aforementioned properties presented maximum values of 176 MPa and 142 MPa at 15wt.% of RHA. The noteworthy performance of the composites in terms of tensile strength can be ascribed to the RHA particles, which act as impediments to dislocation motion and carry the imposed stress in a comparable pattern [28]. The hard RHA particles also hinder the dislocation front from moving forward, thus strengthening the matrix. The considerable enhancement in tensile strength is attributed to the enhanced matrix and higher reinforcement adhesion. However, as the RHA % increased to 15wt.%, the tensile strength was

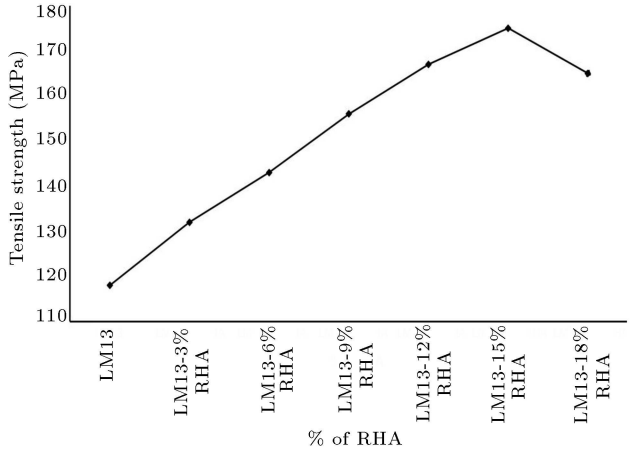

Figure 2. Tensile strength of LM13-RHA composite.

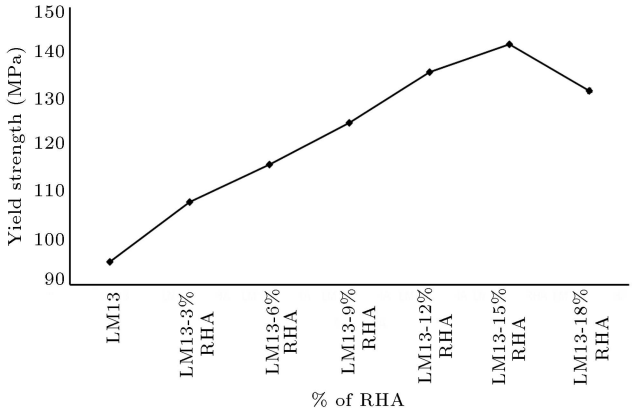

Figure 3. Yield strength of LM13-RHA composite.

reduced owing to agglomeration and segregation of RHA. Similar results were found by Aigbodion and Hassan [29].

4.3. Microstructural analysis

Figure 4 depicts the microstructure of the LM/RHA composites. The microstructure significantly demonstrates the homogeneous distribution of RHA grains and microscopic discontinuities. The ceramic phase was dark, whereas the metal phase was white, and the microstructures of the composites showed excellent persistence of RHA particles. However, there has been aggregation and segregation of RHA particles reinforced with LM13 alloy with 18% RHA particles. These structures match the findings of Aigbodion and Hassan [29] of co-continuous interlaced phases in aluminum alumina needles. These structures are consistent with other researchers' findings [23–26]. The inclusion of a significant of silicon and iron in the matrix phase confirmed that the composite elements examined formed the required bonding. The structure exhibits a eutectic phase in an aluminum matrix containing Fe_3Si, Al_6Fe, etc. The interfaces between the matrix and the particles had an adhesive quality of element bonding because they were free of intermediate

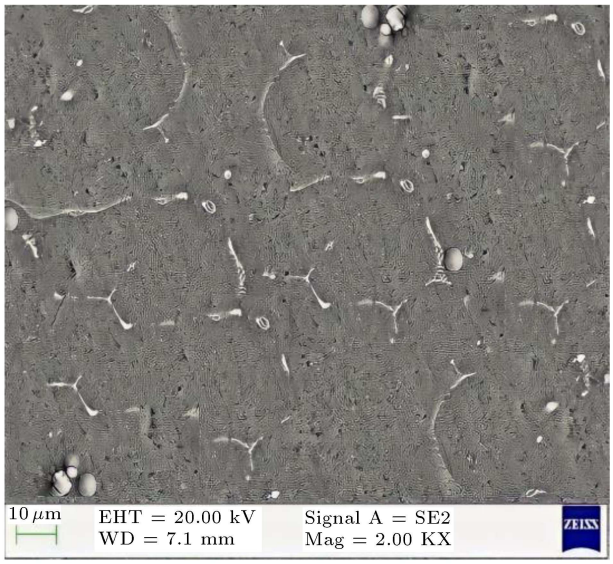

(a)

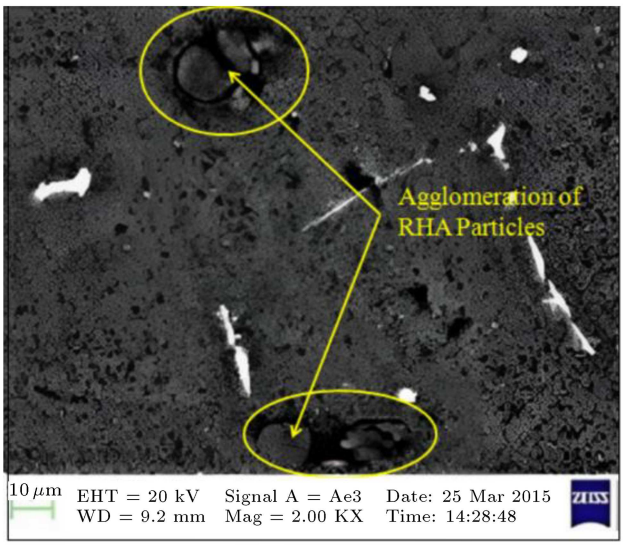

(b)

Figure 4. SEM image (a) (LM/12% RHA and (b) LM/15% RHA composite.

phases and precipitates. Furthermore, they had a high degree of homogeneity (no microcracks) and bonding strength. It agrees with Lakshmikanthan and Prabu findings [30].

4.4. Selection of material for turning operation

It is evident from experimental analysis that LM13-15wt.% shows higher tensile strength and hardness compared to LM13 alloy, and other combinations were investigated. The following factors contributed to an increase in the hardness of LM13-15wt.%RHA: (a) high hardness and density of RHA particles, (b) homogeneous distribution of RHA in the aluminum matrix and (c) a large amount of RHA (ceramic) creates additional dislocations, increasing hardness. The enhancement

Table 4. ANOVA for surface roughness.

Source	Sum of squares	df	Mean square	F-value	p-value (Prob $> F$)	
Block	0.014	1	0.014			
Model	**2.49**	**9**	**0.28**	**600.8**	**< 0.0001**	**Significant**
Aspeed	0.71	1	0.71	1549.67	< 0.0001	
B-feed	0.68	1	0.68	1480.8	< 0.0001	
C-depth of cut	0.42	1	0.42	904.64	< 0.0001	
AB	0.047	1	0.047	101.11	< 0.0001	
AC	0.15	1	0.15	322.83	< 0.0001	
BD	0.12	1	0.12	255.66	< 0.0001	
A^2	0.19	1	0.19	405.82	< 0.0001	
B^2	0.24	1	0.24	512.18	< 0.0001	
C^2	0.022	1	0.022	48.61	< 0.0001	
Residual	0.000414	9	0.000460			
Lack of fit	**0.000304**	**5**	**0.000608**	**2.21**	**0.231**	**Not significant**
Pure error	0.000110	4	0.000275			
Cor total	2.51	19				
R-squared	0.998338					
Adj R-squared	0.996677					
Pred R-squared	0.988902					
Adeq precision	92.03817					

in tensile strength can be ascribed to the LM13 matrix's homogeneous distribution of reinforcements, which minimizes porosity inside the composites and helps to promote uniform load distribution. Based on the experimental analysis, LM13-15wt.%RHA composite specimen got optimum mechanical properties. Therefore, LM13-15wt.%RHA is taken for further machining studies. The turning operation is performed on the selected specimen, and the process parameter is optimized using a multi-objective optimization by RSM.

4.5. Analysis of developed quadratic model

The ANOVA study was carried out to evaluate the created model with 95% confidence intervals and has been reported in Tables 4 and 5. Regression model significance testing, individual model coefficient significance testing, and incompatibility testing are all performed with the statistical tool. The regression model automatically eliminates insignificant model terms. The acceptable reliability measures R^2, adjusted R^2, and predicted R^2 are shown in Table 4 and 5. The quality of fit of the models is measured using the R^2 degree of confidence, which assesses how much variance in measured predicted values can be attributed to controllable factors. All R^2 regression equations are essentially equal to 1 in this case. [31].

Tables 4 and 5 highlight the ANOVA for surface roughness and MRR. Since the 'p' ('Prob. $> F$") result is less than 0.05 (i.e., $a = 0.05$, or 95% confidence), the created models are statistically significant, which is desired because it indicates that the model terms have a substantial influence on the response. The degree of compatibility is measured by the ratio of variance to overall variation (R^2) [32]. The prediction coefficients are the term coined for this finding in the ANOVA tables.

A higher R^2 value indicates a better fit between the model and the data. R^2 values for surface roughness and MRR are 0.998 and 0.998, which are close to unity, demonstrating the model is adequate [33,34]. The following are the final quadratic response equations for MRR and surface roughness.

$$\begin{aligned} Surface\ Roughness\,(SR) = {} & +2.63 + (0.27 \times A) \\ & + (0.26 \times B) + (0.20 \times C) - (0.076 \times A \times B) \\ & + (0.14 \times A \times C) - (0.12 \times B \times C) \\ & - \left(0.26 \times A^2\right) + (0.30 \times B^2) + (0.091 \times C^2), \end{aligned} \quad (2)$$

$$\begin{aligned} Metal\ Removal\ Rate\ (MRR) = {} & +1568.68 \\ & + (70.50 \times A) - (153.00 \times B) - (22.50 \times C) \end{aligned}$$

Table 5. ANOVA for Metal Removal Rate (MRR).

Source	Sum of squares	df	Mean square	*F*-value	*p*-value (Prob > *F*)	
Block	35191.88	1	35191.88			
Model	**1.05E+06**	**9**	**1.17E+05**	**610.79**	**< 0.0001**	**Significant**
A-speed	49702.5	1	49702.5	259.91	< 0.0001	
B-feed	2.34E+05	1	2.34E+05	1224.12	< 0.0001	
C-depth of cut	5062.5	1	5062.5	26.47	0.0006	
AB	1.01E+05	1	1.01E+05	529.46	< 0.0001	
AC	1.54E+05	1	1.54E+05	805.37	< 0.0001	
BC	4.85E+05	1	4.85E+05	2536.77	< 0.0001	
A^2	754.41	1	754.41	3.95	0.0783	
B^2	12877.77	1	12877.77	67.34	< 0.0001	
C^2	470.2	1	470.2	2.46	0.1513	
Residual	1721.09	9	191.23			
Lack of fit	**815.59**	**5**	**163.12**	**0.72**	**0.6421**	**Not significant**
Pure error	905.5	4	226.38			
Cor total	1.09E+06	19				
R-squared	0.9984					
Adj R-squared	0.9967					
Pred R-squared	0.9899					
Adeq Precision	99.799					

$$+(112.50 \times A \times B) - (138.75 \times A \times C) - (246.25 \times B \times C) - \left(16.76 \times A^2\right) - \left(69.26 \times B^2\right) + \left(13.24 \times C^2\right). \quad (3)$$

4.6. Residual plot

Residual analysis has also been used as a major analytical tool to assess the adequacy of results. Figure 5(a)–(d) shows a normal probability map of residuals for surface roughness and MRR. The straight line connects all the data points, indicating a strong connection between the projected model and experimental values. As a result, the data is disseminated normally. Figure 5(a)–(d) demonstrates this. It aids in detecting a value, or a group of values, that the model is unable to predict. The figure indicates that most values are concentrated on the 45° line; hence, the model assumptions are correct [35]. As a result, the created second-order mathematical model may be used to estimate surface roughness while machining LM13-15wt.%RHA composites effectively.

4.7. Output responses (MRR and surface roughness) of process parameters

Figure 6(a)–(c) illustrates the surface roughness and Figure 7(a)–(c) depicts the MRR being recorded as a function of process parameters such as speed and feed, with the third variable being the depth of cut, kept constant in the center. Upon increased cutting speed, surface roughness diminished, and MRR increased simultaneously. The graph shows that the surface roughness at intermediate cutting speed obtained better surface roughness. With an increase in feed rate, surface roughness increases significantly. If the feed rate is raised during machining, the normal loads on the tool will increase as well, generating heat that will increase the surface roughness [36]. Figure 6(a)–(c) demonstrates a 3-D surface graph, and Figure 7(a)–(c) illustrates a 3-D MRR plot for the effect of cutting speed on cut depth when the feed is kept at an intermediate level. In the machining of LM13/RHA composites, increasing the depth of cut has no discernible effect on surface roughness, whereas MRR increases. The better surface roughness could only be attained at the maximum level of depth of cut, as shown in Figure 6. It could be due to material inhomogeneity, in-house fabrication, machine tool setup, cutting tool use, machine tool vibration, and other factors [37].

4.8. Desirability analysis

The desirability of output parameters is depicted in

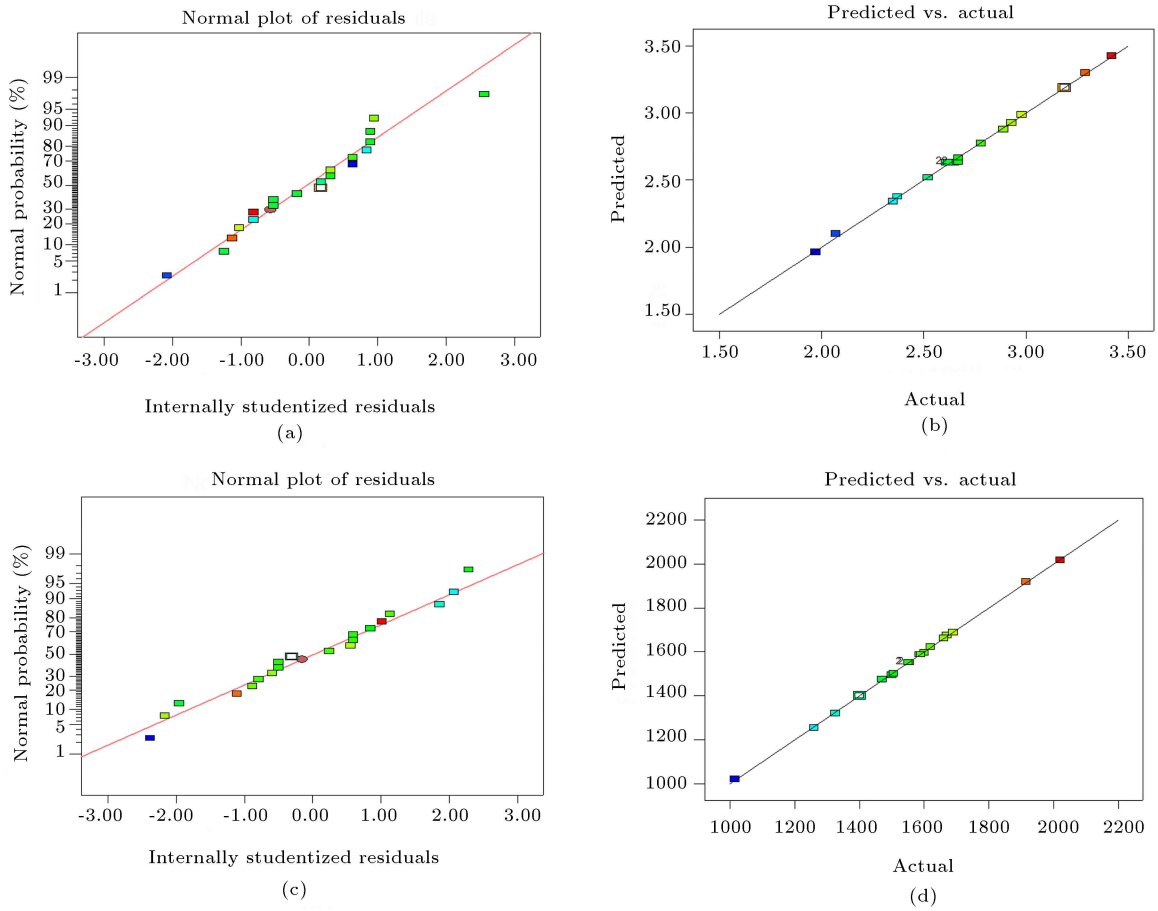

Figure 5. (a) Normal probability plot, (b) predicted vs. actual plot for surface roughness, (c) normal probability plot, and (d) predicted vs. actual plot for MRR.

graphs of the ramp function and the bar chart shown in Figure 8(a) and (b). The process parameters or response analysis for that response characteristic is represented by the pointer on each ramp. The size of the pointer indicates how valuable it is. A regression ramp function was generated among the minimal value and the objective or the maximum value and the objective. Since the weight for every parameter was assigned to one, the total desirability function of the responses is represented by a bar chart. Desirability ranges from 0 to 1, depending on how close the response comes to hitting the target. The graph demonstrates how each parameter fits the requirement, with values around one regarded as good [38].

The optimal value of the turning parameters was obtained from desirability analysis and is as follows: cutting speed of 750 rpm, feed 0.1 mm/rev, and depth of cut 0.3 mm. A higher level of lower speed, lower feed, and deeper cut minimizes surface roughness and maximises MRR for the produced composite. The obtained desirability value for all turning parameters is 0.863, and for output response, the value of desirability for surface roughness is 0.71663; for MRR, it is 0.747491, and combined desirability is 0.731898.

4.9. Validation of experiments

Validation experiments are used to validate the parameters of the model and optimize condition findings. The validation experiment results are shown in Figure 9. Validation tests were carried out at ideal levels under three conditions (std run 5, 10, and 8, as in Table 3). Based on the study of Figure 9, it can be determined the generated RSM model has a high degree of agreement with experimental results. In addition, the ideal cutting condition minimizes surface roughness and MRR compared to the other studied cutting conditions.

4.10. Sensitivity analysis

Sensitivity analysis is a critical process for identifying and evaluating critical components based on their importance. Model validation is comparing the predicted outcome to the measured data. This study can determine which parameters require the most accurate measure and which input variables significantly impact model outputs [39]. The partial derivative of a design empirical optimization problem to its variables reflects the sensitivity of a function to a design variable in mathematics. The sensitivity equations for cutting

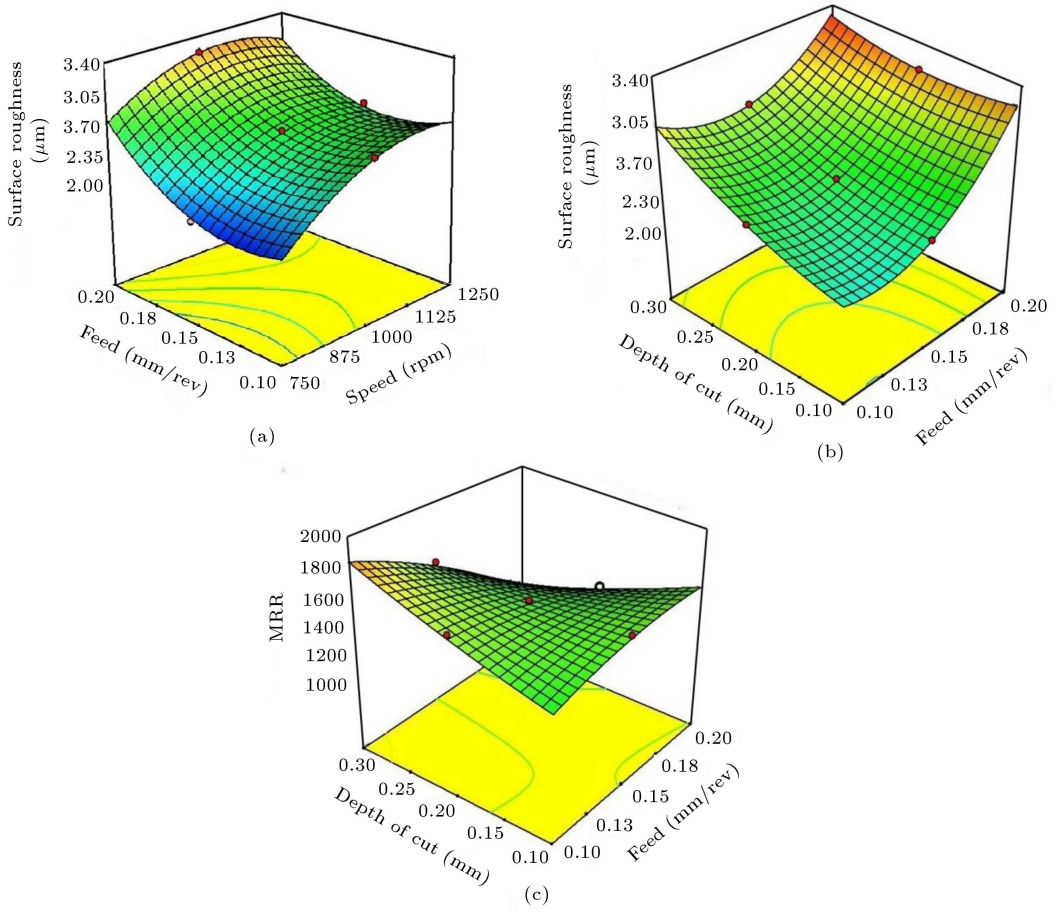

Figure 6. 3D surface plot for surface roughness.

speed are obtained by differentiating Eqs. (4) to (9) with respect to cutting speed. The letter E stands for sensitivity.

$$\frac{\delta R_a}{\delta \mathrm{A}} = +0.27 - (0.076 \times B) + (0.14 \times C) - (0.52 \times \mathrm{A}), \quad (4)$$

$$\frac{\delta R_a}{\delta B} = +0.26 - (0.076 \times \mathrm{A}) - (0.12 \times C) + (0.60 \times B), \quad (5)$$

$$\frac{\delta R_a}{\delta C} = +0.20 + (0.14 \times A) - (0.12 \times B) + (0.182 \times C), \quad (6)$$

$$\frac{\delta MRR}{\delta \mathrm{A}} = +70.50 + (112.50 \times B) - (138.75 \times C) - 33.52 \times A), \quad (7)$$

$$\frac{\delta MRR}{\delta \mathrm{B}} = -153.00 + (112.50 \times A) - (246.25 \times C) - (138.52 \times B), \quad (8)$$

$$\frac{\delta MRR}{\delta C} = -22.50 + (138.75 \times A) - (246.25 \times B) - (26.48 \times C). \quad (9)$$

The sensitivity Eqs. (4)–(9) represent the sensitivity of surface roughness and MRR for cutting speed, feed, and depth of cut, respectively. This research aims to anticipate the tendency of surface roughness and MRR owing to changes in machining process parameters. A positive sensitivity number shows that increasing design parameters leads to a higher objective function, while a negative value implies the contrary. Table 6 and Figure 10(a) and (b) show the sensitivity of surface roughness and MRR derived from Eqs. (4)–(9). When the cutting speed is increased, even a slight change in the cutting speed enables huge changes in the MRR and surface roughness. The results show that cutting speed has a greater impact on MRR and surface roughness.

5. Conclusion

The following conclusions are derived from the findings of this research: The LM13-RHA composites are successfully manufactured using the stir-casting pellet

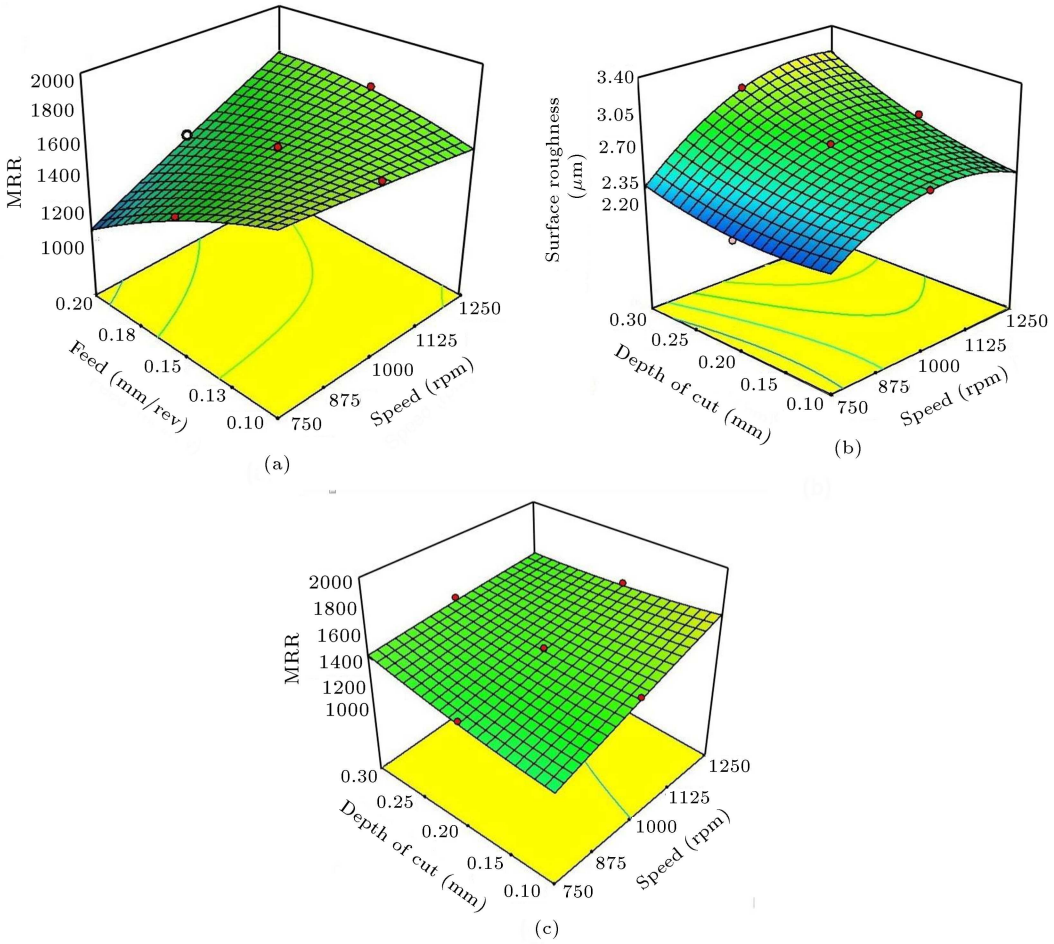

Figure 7. 3D surface plot for MRR.

method by varying the wt.% of Rice Husk Ash (RHA). In addition to reinforcement, the tensile strength, yield strength, and hardness values increase. The inclusion of a significant amount of RHA in the matrix phase confirmed that the composite elements have good bonding strength and a high degree of homogeneity, which is

Table 6. Surface roughness and MRR sensitivities of processes parameters (feed (mm/rev) = 0.15).

Depth of cut (mm)	Cutting speed (RPM)	Sensitivity					
C	A	$\frac{\delta R_a}{\delta A}$	$\frac{\delta R_a}{\delta B}$	$\frac{\delta R_a}{\delta C}$	$\frac{\delta MRR}{\delta A}$	$\frac{\delta MRR}{\delta B}$	$\frac{\delta MRR}{\delta C}$
0.1	750	0.65	0.46	0.24	242.77	−19.25	89.77
	1000	1.46	0.38	0.38	209.25	93.25	−48.98
	1250	−0.39	0.30	0.52	175.73	205.76	−187.73
0.2	750	0.79	0.34	0.06	104.02	−265.50	116.25
	1000	0.27	0.26	0.20	70.50	−153.00	−22.50
	1250	0.34	0.18	0.34	36.98	−40.50	−161.25
0.3	750	0.65	0.22	−0.12	−34.73	−511.76	142.73
	1000	0.41	0.14	0.02	−68.25	−399.25	3.98
	1250	−0.11	0.06	0.16	−101.77	−286.76	−134.77

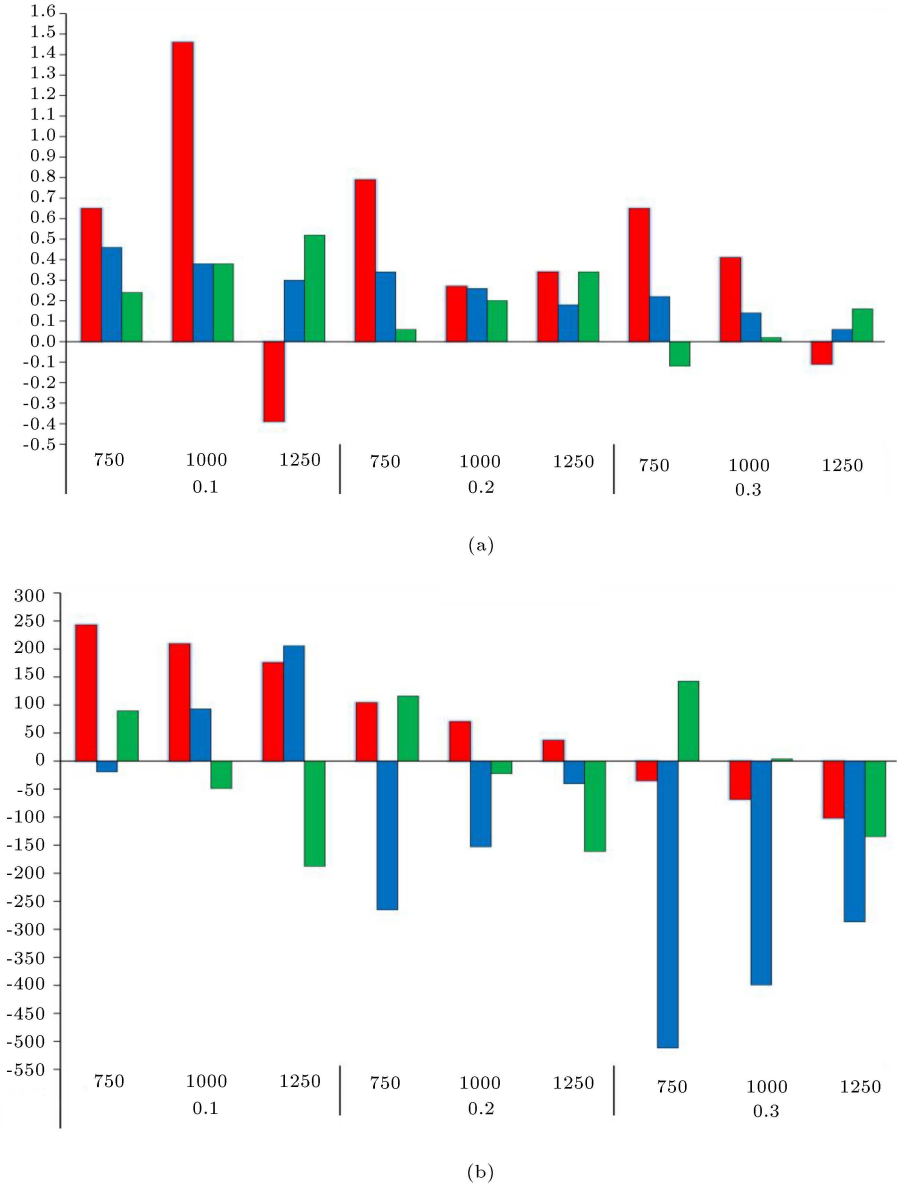

Figure 8. Sensitivity plot for (a) SR and (b) MRR.

confirmed by Scanning Electron Microscope (SEM) analysis. The structure exhibits a eutectic phase in an aluminum matrix containing Fe_3Si, Al_6Fe, etc. To create superior requisite qualities, RHA addition should be between 10–15% for excellent service performances of this alloy. Based on the experimental analysis LM13-15wt.%RHA composite specimen got optimum mechanical properties. Therefore, LM13-15wt.%RHA has been considered for machining studies.

Using response surface methods, a functional relation is established between the output response and cutting parameters. Within the parameters investigated, the empirical relationship developed can identify Material Removal Rate (MRR) and surface roughness in the machining of LM13-15wt.%RHA composite. ANOVA results and validation experiments have demonstrated that mathematical models of experiments and predicted values of responses are close to those measured experimentally with a 95% confidence interval. A desirability-based method is used to optimize cutting parameters for the machining of composite. Within the criteria analyzed, the ideal settings minimize surface roughness and maximize MRR in composite machining. A sensitivity analysis was performed, and it was found that cutting speed significantly impacts the responses studied. Based on the findings, LM13-RHA composites have proven to be a promising material where the lightweight, high strength, and hardness, with low machining costs, are primary requirements; examples of real-world applications could be in pistons, liners, calipers, and brake rotors.

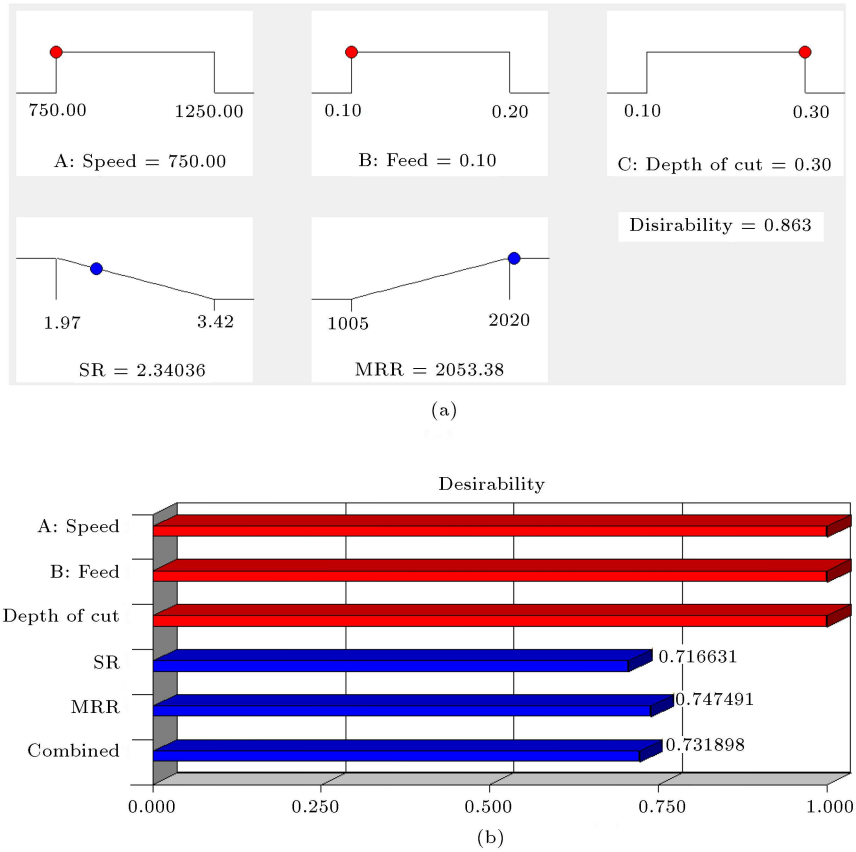

Figure 9. (a) Ramp function plot of desirability; (b) Ramp function bar plot of desirability.

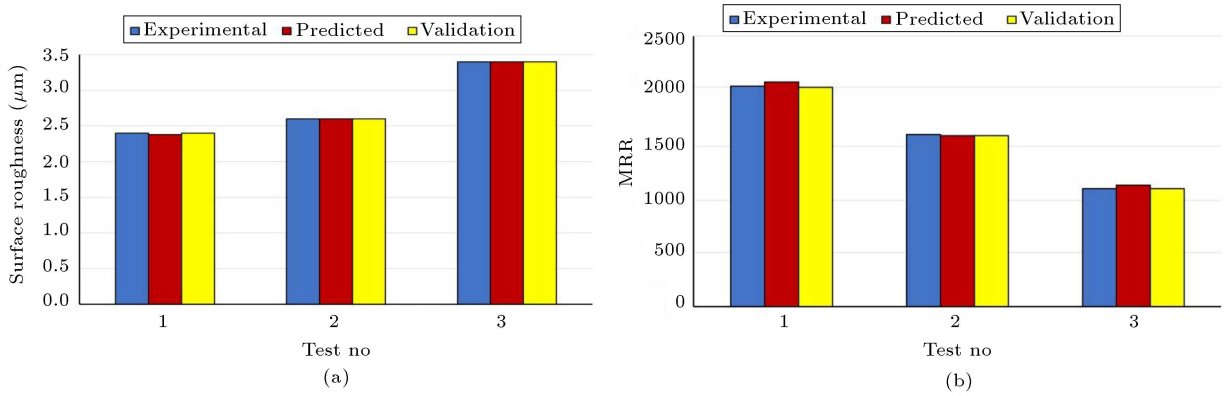

Figure 10. Validation plot for (a) Surface Roughness (b) MRR.

References

1. Ajay Kumar, P., Rohatgi, P., and Weiss, D. "50 years of foundry-produced metal matrix composites and future opportunities", *Int J Met*, **14**(2), pp. 291–317 (2020).

2. Suthar, J. and Patel, K.M. "Processing issues, machining and application of aluminum metal matrix composites", *Mater. Manuf. Processes*, **33**(5), pp. 499–527 (2018).

3. Jose, J., Christy, T.V., Peter, P.E., et al. "Manufacture and characterization of a novel agro-waste based low-cost Metal Matrix Composite (MMC) by compocasting", *Mater. Res. Express*, **5**(6), 066530 (2018).

4. Panwar, N. and Chauhan, A. "Fabrication methods of particulate reinforced aluminium metal matrix, composite-A review", *Mater. Today*, **5**, pp. 5933–5939 (2018).

5. Natarajan, N., Vijayarangan, S., and Rajendran, I. "Wear behaviour of A356/25SiC aluminium matrix composites sliding against automobile friction material", *Wear*, **261**, pp. 812–822 (2006).

6. Zhang, C., Yao, D., Yin, J., et al. "Microstructure and mechanical properties of Aluminium matrix com-

posites reinforced with pre-oxidized βSi_3N_4 whiskers", *Mater. Sci. Eng. A*, **723**, pp. 109–117 (2018).

7. Ochieze, B.Q., Nwobi-Okoye, C.C., and Atamuo, P.N. "Experimental study of the effect of wear parameters on the wear behavior of A356 alloy/cow horn particulate composites", *Def. Technol.*, **14**, pp. 77–82 (2018).
8. Bodunrin, M.O., Alaneme, K.K., and Chown, L.H. "Aluminium matrix hybrid composites: A review of reinforcement philosophies; Mechanical, corrosion and tribological characteristics", *J. Mater. Res. Technol.*, **4**, pp. 434–445 (2015).
9. Alaneme, K.K. and Olubambi, P.A. "Corrosion and wear behaviour of rice husk ash-Alumina reinforced Al-Mg-Si alloy matrix hybrid composites", *J. Mater. Res. Technol*, **2**(2), pp. 188–194 (2013).
10. Allwyn Kingsly Gladston, I., Dinaharan, N., Mohamed Sheriff, J., et al. "Dry sliding wear behavior of AA6061 aluminum alloy composites reinforced rice husk ash particulates produced using compocasting", *J. Asian Ceram. Soc.*, **5**(2), pp. 127–135 (2017).
11. Sivaprasad, D. and Krishna, A.R. "Effect of T6 heat treatment on damping characteristics of Al/RHA composites", *Bull. Mater. Sci*, **35**(6), pp. 989–995 (2012).
12. Monaghan, J.M. "The use of quick stop test to study the chip formation of an SiC/Al metal matrix composite and its matrix alloy", *Process Adv Mater*, **4**, pp. 170–179 (1994).
13. Sahin, Y., Kok, M., and Celik, H. "Tool wear and surface roughness of Al_2O_3 particle-reinforced aluminium alloy composites", *J. Mater. Process. Technol*, **128**(1–3), pp. 280–291 (2002).
14. Hocheng, H., Yen, S.B., Ishihara, T., et al. "Fundamental turning characteristics of a tribology-favored graphite/aluminium alloy composite material", *Compos. Part A Appl. Sci. Manuf*, **28**(9–10), pp. 883–890 (1997).
15. Hung, N.P., Yeo, S.H., Lee, K.K., et al. "Chip formation in machining particle-reinforced metal matrix composites", *Mater. Manuf. Process*, **13**(1), pp. 85–100 (1998).
16. Krishnamurthy, L. and Sridhara, L.K. "Comparative study on the machinability aspects of aluminium-silicon carbide and aluminium graphite- silicon carbide hybrid composites", *Int. J. Mach. Mach. Mater*, **10**(2), pp. 137–152 (2011).
17. Alaneme, K.K. and Ajayi, O.J. "Microstructure and mechanical behaviour of stir-cast Zn-27Al based composites reinforced with rice husk ash, silicon carbide, and graphite", *J. King Saud Univ. Eng. Sci*, **27**(2), pp. 172–177 (2017).
18. Alaneme, K.K., Adewale, T.M., and Olubambi, A.P. "Corrosion and wear behaviour of Al-Mg-Si alloy matrix hybrid composites reinforced with rice husk ash and silicon carbide", *J. Mater. Res. Technol*, **3**(1), pp. 9–16 (2013).
19. Sankhla, A. and Patel, K.M. "Metal matrix composites fabricated by stir casting process-a review", *Adv. Mater. Process. Technol*, **8**(2), pp. 1–22 (2021).
20. Radhika, N. and Raghu, R. "Prediction of mechanical properties and modeling on sliding wear behavior of LM25/TiC composite using response surface methodology", *Part. Sci. Technol.*, **36**(1), pp. 1–8 (2018).
21. Vettivel, S.C., Selvakumar, N., Narayanasamy, R., et al. "Numerical modelling, prediction of Cu-W nano powder composite in dry sliding wear condition using response surface methodology", *Mater. Des.*, **50**, pp. 977–96 (2013).
22. Mishra, A.K., Sheokand, R., and Srivastava, R.K. "Tribological behaviour of Al6061/SiC metal matrix composite by Taguchi's Techniques", *Int. J. Sci. Res.*, **2**(10), pp. 1–8 (2012).
23. Kumar, N.S., Ravindranath, V.M., and Shankar, G.S. "Mechanical and wear behaviour of aluminium metal matrix hybrid composites", *Procedia Mater. Sci*, **5**, pp. 908–917 (2014).
24. Babu, K.A. and Jeyapaul, R. "An investigation into the wear behaviour of a hybrid metal matrix composite under dry sliding conditions using Taguchi and ANOVA methods", *Journal of Bio- and Tribo-Corrosion*, **8**(1), pp. 1–12 (2022).
25. Yallese, M.A., Chaoui, K., Zeghib, N., et al. "Hard machining of hardened bearing steel using cubic boron nitride tool", *J. Mater. Process. Technol.*, **209**, pp. 1092–1104 (2009).
26. Rajan T.P.D., Pillai, R.M., Pai, B.C., et al. "Fabrication and characterization Al-7Si-0.35Mg/fly ash metal matrix composites processed by different stir casting routes", *Compos Sci Technol*, **67**, pp. 3369–3377 (2007).
27. Aigbodion, V.S. "Potential of using bagasse ash particle in metal matrix composite", PhD dissertation, department of metallurgical and materials engineering, Ahmadu Bello University, Samaru, Zaria, Nigeria, pp. 34–50 (2010).
28. Lakshmikanthan, P. and Prabu, B. "Mechanical and tribological behaviour of aluminium Al6061-coconut shell ash composite using stir casting pellet method", *J. Balk. Tribol. Assoc*, **22**, pp. 4008–4018 (2016).
29. Aigbodion, V.S. and Hassan, S.B. "Effects of silicon carbide reinforcement on microstructure and properties of cast Al-Si-Fe/SiC particulate composites", *J. Mater. Sci. Eng. A*, **447**, pp. 355–360 (2007).
30. Lakshmikanthan, P. and Prabu, B. "Wear and corrosion behavior of Coconut Shell Ash (CSA) reinforced Al6061 metal matrix composites", *Mater. Test*, **62**(1), pp. 77–84 (2020).
31. Shankar, S., Balaji, A., and Pramanik, A. "Optimization of turning parameters for AlSi10Mg/SCBA/SiC hybrid metal matrix composite using response surface methodology", *Mater. Res. Express*, **6**(10), 106553 (2019).
32. Dandekar, R.C. ans Shin, Y.C. "Modeling of machining of composite materials: a review", *Int. J. Mach. Manuf.*, **57**, pp. 102–123 (2012).

33. Rajmohan, T. and Palanikumar, K. "Experimental investigation and analysis of thrust force in drilling hybrid metal matrix composites by coated carbide drills", *J. Mater. Manuf. Process.*, **26**, pp. 961–968 (2011).

34. Joardar, N., Das, S., Sutradhar, G., et al. "Application of response surface methodology for determining cutting force model in turning of LM6/SiCP metal matrix composite", *Meas*, **47**, pp. 452–464 (2014).

35. Palanikumar, K. and Karthikeyan, R. "Assessment of factors influencing surface roughness on the machining of Al/SiC particulate composites", *Mater. Des*, **28**, pp. 1584–1591 (2007).

36. Adalarasan, R., Santhanakumar, M., and Rajmohan, M. "Optimization of laser cutting parameters for Al6061/SiCp/Al_2O_3 composite using grey based response surface methodology (GRSM)", *Meas*, **73**, pp. 596–606 (2015).

37. Palanikumar, K. "Application of Taguchi and response surface methodologies for surface roughness in machining glass fiber reinforced plastics by PCD tooling", *Int. J. Adv. Manuf. Technol.*, **36**(1), pp. 19–27 (2008).

38. Palanikumar, K., Muthukrishnan, N., and Hariprasad, K.S. "Surface roughness parameters optimization in machining A356/Sic/20p metal matrix composites by PCD tool using response surface methodology and desirability function", *Mach. Sci. Technol.*, **12**, pp. 529–545 (2008).

39. Kim, I.S., Son, K.J., Yang, Y.S., et al. "Sensitivity analysis for process parameters in GMA welding processes using a factorial design method", *Int. J. Mach. Tools Manuf*, **43**, pp. 763–769 (2003).

Biographies

Purushothaman Lakshmikanthan completed his undergraduate in Mechanical Engineering, M. Tech in Product Design and Manufacturing specialization, and a PhD degree from Pondicherry Engineering College. He is currently employed at the University College of Engineering, Panruti. Throughout his teaching career, he has gained 13 years of experience. He has published in various national and international journals and conferences. His area of expertise is Manufacturing and composite materials.

Krishnamurthy Senthilvel works as a Lecturer (Sel. grade) in Karaikal Polytechnic College, Govt. of Puducherry. He has done his B. Tech from Pondicherry Engineering College and M. Tech from Guindy Engineering College, Anna University, Chennai. He has completed his PhD in the Department of Mechanical Engineering, Pondicherry Engineering College, on Hybrid nanocomposites in rubber for oil seal applications. He has published 15 research papers in international journals and conferences.

Balakrishnan Prabu is working as a Professor in the Department of Mechanical Engineering at Pondicherry Engineering College. He has done his M. Tech (Design) from Guindy Engineering College, Anna University, Chennai, and PhD from the Department of Mechanical Engineering, Pondicherry Engineering College. His area of expertise is engineering design and finite element analysis. He has guided 3 PhD students. He has Published 65 research papers in international journals and conferences.